Atmospheric Nonequilibrium Plasma Treatment of Biaxially Oriented Polypropylene

R. D. Boyd, A. M. Kenwright, and J. P. S. Badyal*

Chemistry Department, Science Laboratories, University of Durham, Durham DH1 3LE, England, U.K.

D. Briggs

ICI plc, Wilton Research and Technology Centre, P.O. Box 90, Middlesbrough, Cleveland TS90 8JE, England, U.K.

Received July 1, 1996; Revised Manuscript Received November 19, 1996[⊗]

ABSTRACT: The chemical and physical effects incurred at the surface of biaxially oriented polypropylene film during silent discharge plasma treatment have been investigated using XPS, NMR, TOF-SIMS, and AFM techniques. It is found that chain scission accompanied by oxidative attack leads to the formation of low molecular weight oxidized material which agglomerates into globules at the surface due to a large difference in interfacial free energy between the underlying hydrophobic substrate and the oxygenated overlayer.

1. Introduction

Nonequilibrium plasmas are widely used to modify the surface properties of plastics and rubbers. For instance, noble gas plasmas are effective at etching polymer surfaces,[1] CF_4 plasmas can lead to surface fluorination,[2,3] whereas oxygen plasma treatment can enhance polymer wettability and adhesion via surface oxidation.[4] Both the chemical and physical changes taking place at the electrical discharge/substrate interface can influence the resultant surface performance.

The chemical nature of plasma-treated polymers has been extensively examined by surface-sensitive analytical techniques, which include X-ray photoelectron spectroscopy (XPS),[5−9] secondary ion mass spectrometry (SIMS),[10] and contact angle measurements.[11] However, plasma modification can penetrate to several microns below the polymer surface,[12] and therefore the sampling depth of such surface-sensitive techniques (which is typically on the order of nanometers) may not necessarily be representative of the whole plasma-modified layer. Here we combine XPS, solution-state NMR analysis, and TOF-SIMS in order to attain a better insight into the chemical composition of the treated surface layer produced during atmospheric dielectric barrier (silent) discharge modification of biaxially oriented polypropylene.

Investigation of the physical changes imparted during plasma treatment has in the past been mainly restricted to scanning electron microscopy (SEM) studies.[13,14] One of the major drawbacks of SEM is that it usually requires insulating samples to be coated with a conductive layer which can mask any plasma-induced surface modification. Furthermore, SEM probes the specimen with a high-energy electron beam, which can damage the polymer surface during analysis. The relatively recent invention of atomic force microscopy (AFM) overcomes the aforementioned limitations of SEM.[15] AFM works by scanning a very sharp tip attached to a lightly sprung cantilever across the sample surface while keeping the repulsive force between the probe and surface constant. Nanometer-scale resolution of nonconducting substrates can routinely be achieved using AFM without the need for any additional sample preparation. Although the morphology of untreated polymer samples has been widely studied by AFM,[16−18] not much attention has been given to the topography of plasma-treated polymers.[19−21]

2. Experimental Section

Atmospheric silent discharge treatments were carried out using a home-built parallel-plate dielectric barrier discharge reactor operating at 3 kHz and 11 kV, with an electrode gap of 3.00 ± 0.05 mm, as shown in Figure 1. Small strips of biaxially oriented polypropylene film (ICI) were washed in a 50/50 mixture of isopropyl alcohol and cyclohexane and dried in air prior to electrical discharge treatment for times ranging from 1 to 300 s.

A Kratos ES300 electron spectrometer equipped with a Mg Kα X-ray source (1253.6 eV) and a concentric hemispherical analyzer was used for XPS analysis. Photoemitted electrons were collected at a take-off angle of 30° from the substrate normal, with electron detection in the fixed retard ratio (FRR, 22:1) mode. XPS spectra were accumulated on an interfaced IBM PC computer. Instrumentally determined sensitivity factors for unit stoichiometry of C(1s):O(1s) were taken as equalling 1.00:0.62. Where error bars are shown, they correspond to the standard deviation calculated from the whole experiment having been repeated at least 3 times.

Solution-state ^{1}H NMR spectroscopy was used to characterize the soluble component of the plasma-

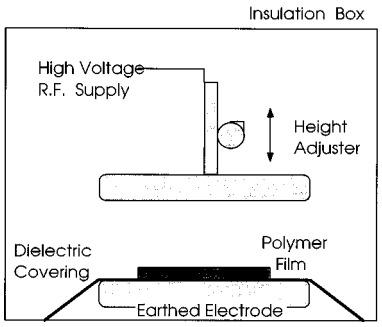

Figure 1. Apparatus used for atmospheric silent discharge treatment of polymer films.

* To whom correspondence should be addressed.
[⊗] Abstract published in *Advance ACS Abstracts,* August 1, 1997.

S0024-9297(96)00940-0 CCC: $14.00

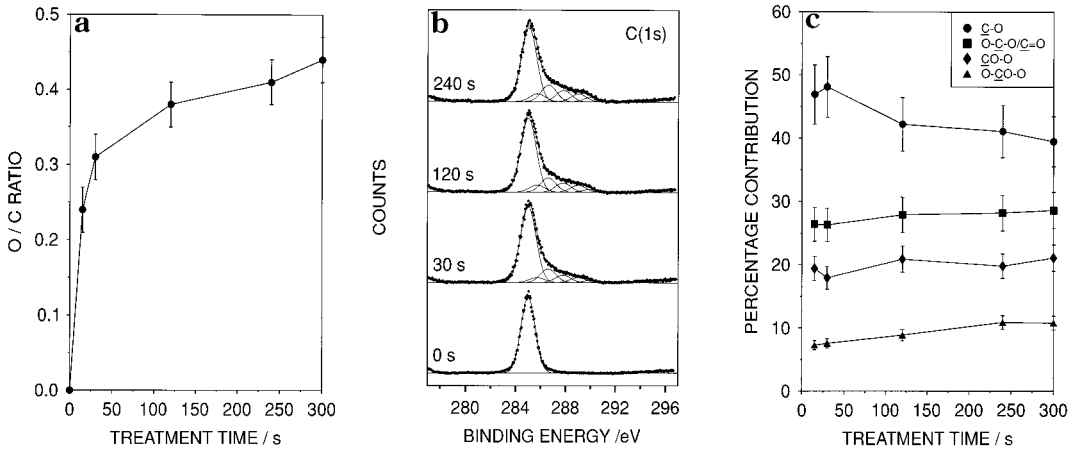

Figure 2. Influence of silent discharge treatment time upon (a) the O/C ratio, (b) C(1s) spectra, and (c) the relative concentration of oxidized carbon moieties ($\Sigma = 100\%$).

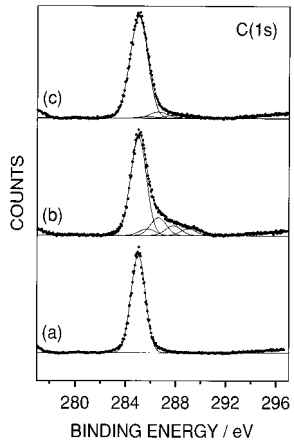

Figure 3. C(1s) XPS spectra of polypropylene: (a) untreated; (b) 30 s silent discharge treatment; (c) silent discharge treatment followed by solvent washing.

modified polymer surface. Approximately 120 cm^2 of polypropylene film was exposed to the dielectric barrier discharge for 120 s in order to generate sufficient soluble material for NMR analysis. Next, the treated layer was extracted from the polypropylene substrate by washing in chloroform solution for a duration of 30 s. Then the chloroform solvent was allowed to evaporate and was replenished with deuterated chloroform prior to analysis by solution-state proton NMR spectroscopy on a Varian VXR-400s spectrometer.

TOF-SIMS analysis was carried out with a Physical Electronics 7200 instrument which has been described previously.[22] The primary ion beam (8 keV Cs^+) with a spot size of ~50 μm was rastered over an area of 100 × 100 μm, keeping the total dose well under 10^{13} ions cm^{-2} (static conditions). In addition to studying the treated film for comparison with XPS data, the material washed from the surface of a few square centimeters of this film was also studied, by deposition onto a substrate, for comparison with NMR data. The chloroform extract was sufficiently concentrated to deposit several monolayers onto a silicon wafer (spin coating) or a submonolayer on nitric acid-etched silver foil in order to generate Ag^+-cationized secondary ions.

A Digital Instruments Nanoscope III atomic force microscope was used to examine the topographical nature of the polypropylene surface prior to and immediately after electrical discharge exposure. All of the AFM images were acquired in air using the Tapping mode,[23] and are presented as unfiltered data. This technique employs a stiff silicon cantilever oscillating at a large amplitude near its resonance frequency (several hundred kilohertz). The large root-mean-square amplitude is used to overcome the capillary attraction of the surface layer, while the high oscillation frequency allows the cantilever to strike the surface many times before being displaced laterally by one tip diameter. These features offer the advantage of low contact forces and negligible shear forces.

Table 1. Relative Peak Intensities of the Oxidized Carbon Peaks ($\Sigma = 100\%$) for 30 s Silent Discharge-Treated Polypropylene: before and after Solvent Washing

sample	$\underline{C}$−O	O−$\underline{C}$−O/$\underline{C}$=O	$\underline{C}$O−O	−O−$\underline{C}$O−O−
unwashed	48 ± 3	26 ± 2	18 ± 2	8 ± 1
washed	53 ± 3	26 ± 2	15 ± 2	6 ± 1

3. Results

3.1. X-ray Photoelectron Spectroscopy. XPS was used to follow the rise in O/C ratio at the polymer surface with increasing silent discharge treatment duration (Figure 2a). A gradual leveling off was evident after 120 s plasma exposure. C(1s) XPS spectra were fitted with Gaussian peaks of equal full width at half-maximum (FWHM),[24] using a Marquardt minimization computer program. Untreated polymer exhibits a single C(1s) peak which corresponds to C_xH_y functionalities (i.e. −CH, $-CH_2$, and $-CH_3$ groups). Silent discharge modification led to the appearance of a shoulder at higher binding energies, which was taken as being indicative of the buildup of oxygenated carbon centers (Figure 2b); this is consistent with the observed variation in the O/C ratio. Binding energies distinctive of different types of oxidized carbon moieties[25] were referenced to the hydrocarbon peak ($-\underline{C}_xH_y-$) at 285.0 eV: carbon adjacent to a carboxylate group ($>\underline{C}-CO_2-$) at 285.7 eV, carbon singly bonded to one oxygen atom ($>\underline{C}-O-$) at 286.6 eV, carbon singly bonded to two oxygen atoms or carbon doubly bonded to one oxygen atom ($-O-\underline{C}-O-/>\underline{C}=O$) at 287.9 eV, carboxylate groups ($-O-\underline{C}=O$) at 289.0 eV, and carbonate carbons ($-O\underline{C}O-O-$) at 290.4 eV. The relative concentration of the $>\underline{C}-O-$ component passes through a maximum around 30 s of treatment (Figure 2c); this subsequent fall in intensity can be attributed to $>\underline{C}-O-$ groups undergoing further oxidation following the initial stages of reaction to more highly oxidized species.[26]

Washing a 30 s silent-discharge-treated polypropylene sample for 5 s in a 50/50 mixture of isopropyl alcohol/cyclohexane resulted in a drop in the O/C ratio from 0.31

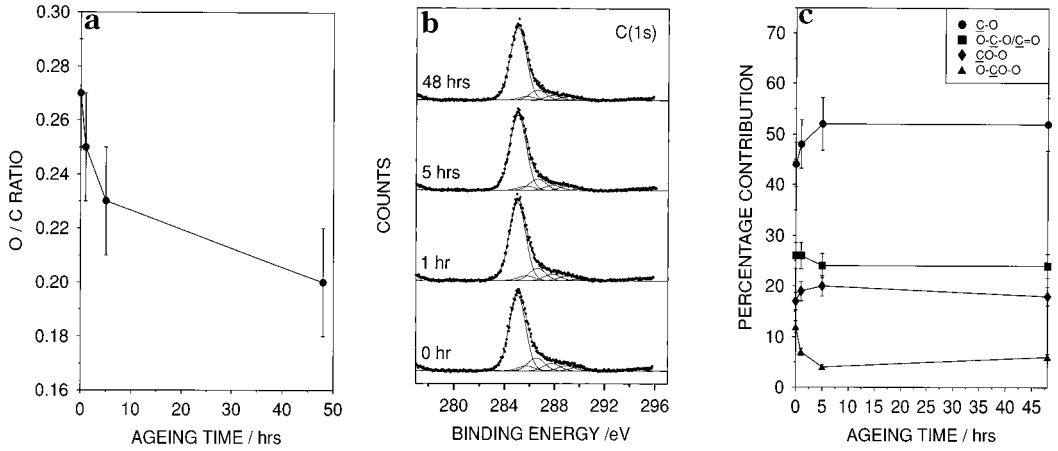

Figure 4. Influence of aging time for a 30 s silent-discharge-treated polypropylene film: (a) O/C ratio; (b) C(1s) spectra; (c) relative concentration of oxidized carbon moieties ($\Sigma = 100\%$).

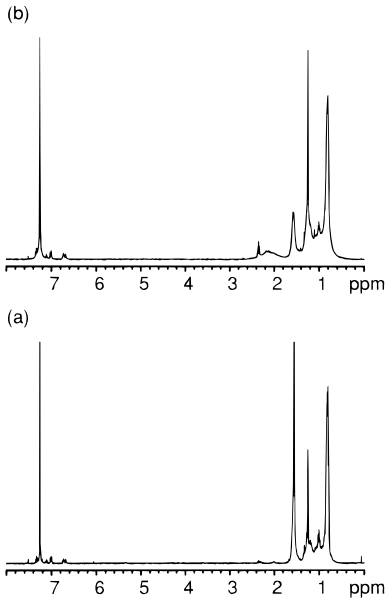

Figure 5. Solution-state proton NMR spectra of (a) washed species from untreated polypropylene and (b) washed species from 120 s silent discharge treated polypropylene.

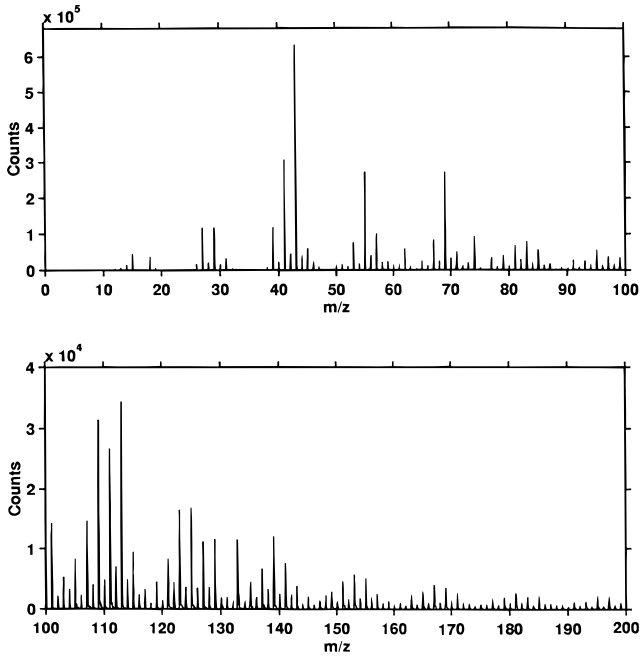

Figure 6. Positive TOF-SIMS of polypropylene silent discharge treated for 30 s.

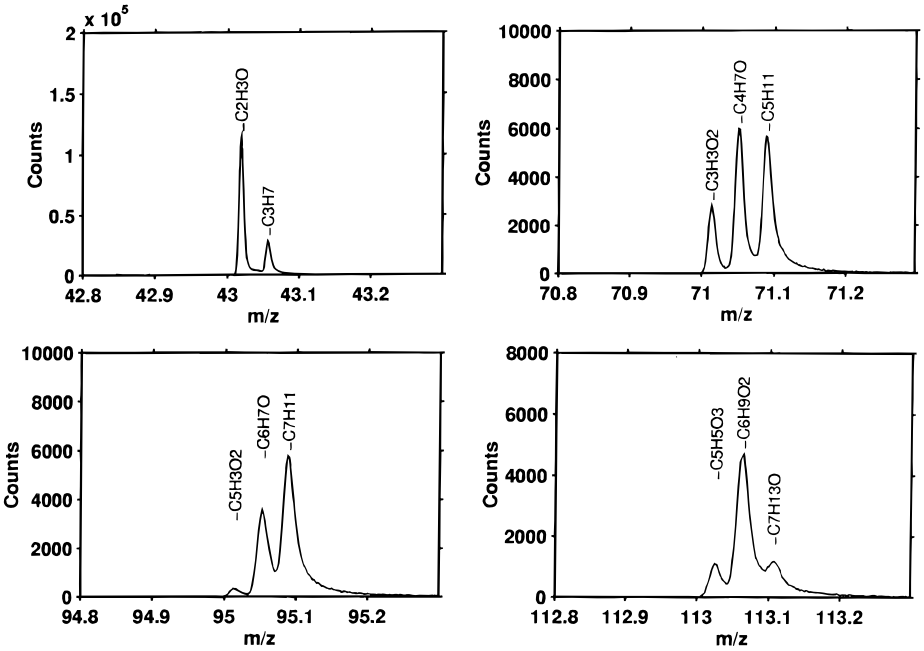

Figure 7. Resolved components of selected peaks from Figure 6.

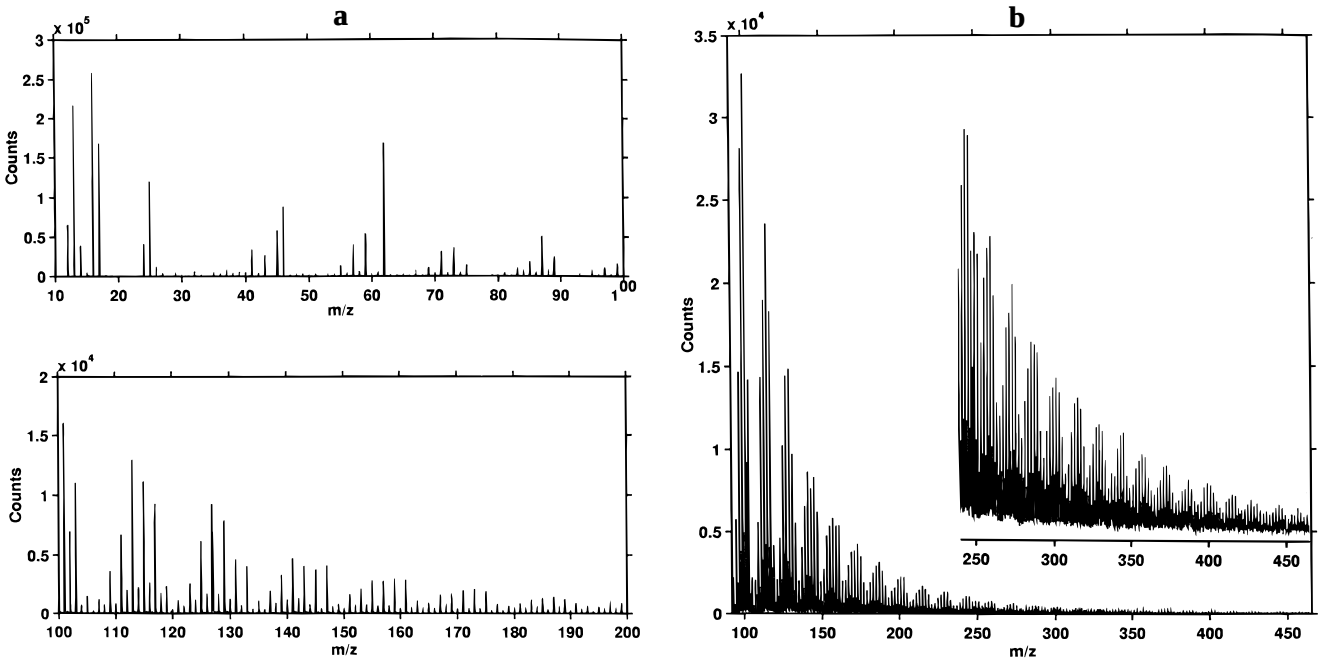

Figure 8. Negative TOF-SIMS of polypropylene silent discharge treated for 30 s: (a) *m*/*z* 10−200 range; (b) *m*/*z* 100−450 range.

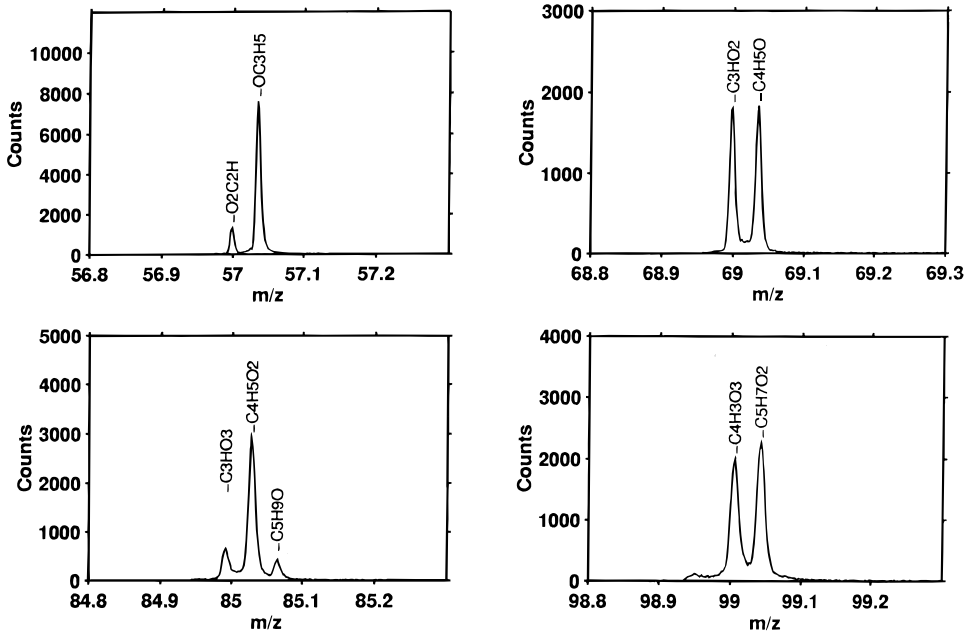

Figure 9. Resolved components of selected peaks from Figure 8a.

± 0.03 to 0.09 ± 0.01 (Figure 3), thereby proving that a large proportion of the modified polymer is weakly bound to the surface. However, it is interesting to note that the relative distribution amongst the oxidized moieties does not differ significantly between the washed and unwashed plasma-treated samples Table 1.

Aging studies showed that the oxidized layer gradually disappears with time. This is evident from the fall in the O/C ratio and the corresponding attenuation of the high binding energy shoulder in the C(1s) envelope with aging time (Figure 4). Carbonate species are lost from the surface at a much faster rate in comparison to the other types of oxidized carbon functionalities.

3.2. Solution-State ^{1}H NMR. Solution-state ^{1}H NMR spectra were taken of the species washed off with chloroform for both untreated and silent-discharge-treated polypropylene (Figure 5). A small amount of residual nondeuterated chloroform is evident in the recorded spectra at 7.3 ppm, this being typical of commercially available deuterated chloroform solvent.[27]

The NMR spectrum of the washed off species from untreated polypropylene consists of two sets of peaks. The first group covers a broad range from 0.8 to 1.6 ppm and corresponds to protons attached to $-CH_3$, $-CH_2$, and $-CH$ groups, which can primarily be attributed to washed out atactic polypropylene.[28] This is not too surprising, since, during the industrial manufacture of biaxially oriented blown polypropylene film, the majority of polymer is present in the isotactic state, with a small amount in the atactic form (98% isotactic, 2% atactic in this case). Atactic polypropylene produced in this way tends to have a lower molecular weight and does not crystallize (i.e., it is located in the amorphous (more mobile) regions of the film); hence, it is much more soluble compared to its isotactic counterpart; i.e., the former can be washed out with chloroform despite being

present in very low concentrations. The sharp peak at 1.6 ppm is characteristic of water residue present in the chloroform solvent. The second set of ^{1}H NMR peaks comprises two weak groupings at 6.7 and 7.1 ppm which correspond to protons bonded to vinylic or aromatic carbons.[29] These are most likely to originate from trace amounts of antioxidants added to the polypropylene film during manufacture.[30] The intensity of the antioxidant features is small compared to those from the atactic polypropylene, thereby suggesting that the majority of the washed out species must be atactic polypropylene.

Solution-state ^{1}H NMR analysis of the chloroform wash taken from the silent-discharge-treated polypropylene surface shows that the distribution of peaks in the 0.6−2.3 ppm region has changed; this is most likely due to some isotactic polymer containing species also being removed,[31] which leads to an overlap with the previously observed atactic features. The water peak at 1.6 ppm has become much broader as a result of hydrogen bonding between the water and washed off low molecular weight oxidized material (LMWOM). In addition, a broad feature is discernible between 1.8 and to 2.4 ppm; this can be attributed to H atoms bonded to an sp^3 carbon center adjacent to an oxygen atom (i.e., alcohols, ethers, esters, etc.).

3.3. TOFSIMS. The positive ion survey scan of the treated film (Figure 6) is at first sight relatively unchanged with respect to that expected from the untreated polypropylene.[32] However, closer inspection of the peaks at any nominal mass reveals oxygenated fragments in addition to the original hydrocarbon ($C_xH_y^+$) only peaks. Some examples are shown in Figure 7. The peak at *m/z* 113 is not a feature of the polypropylene spectrum, consistent with all the components being due to oxygen-containing fragment ions. The peak assignments are from exact mass measurement and are within ∼20 ppm of the calculated masses.

An even more striking change is seen in the negative ion spectrum (Figure 8). The untreated surface gives only C_1^- and C_2^- clusters (*m/z* 12−14 and 24−26, respectively).[32] The expected atomic peaks due to O^-/OH^- (*m/z* 16 and 17) following treatment are accompanied by NO_2^- and NO_3^- (*m/z* 46 and 62) and an extensive series of fragment clusters extending up to nearly *m/z* 500. These are all ions with the general structure $C_xH_yO_z^-$. Some examples are given in Figure 9 for the mass range *m/z* < 100. At higher masses the pattern of peaks in the clusters repeating every 14 amu (CH_2) is very similar (Figure 8b). One representative set is shown in Figure 10. Within this set there are fragments with the generic formulas $C_6O_5H_n^-$, $C_7O_4H_n^-$, $C_8O_3H_n^-$ and possibly $C_5O_6H_n^-$ and $C_9O_2H_n^-$ (weaker components). Because of the greater degree of components overlapping at higher mass, the assignment of the weaker components becomes increasingly uncertain. Overall, the SIMS spectra from the treated surface confirm the very high O/C ratio seen in XPS. It is interesting to note that the negative ion spectrum contains unambiguous contributions from CO_3^- and HCO_3^- (*m/z* 60 and 61). This helps to confirm the assignment of the highest binding energy C(1s) component.

For untreated polypropylene, all the prominent peaks in the spectra obtained from the extract deposited on silicon corresponded to those from polypropylene or the antioxidant Irganox 1076[32] (the $C_xH_yO_z^{\pm}$ peaks were very weak compared to the spectra measured for the plasma-treated polymer surface).

Submonolayer deposition onto silver of the extract taken from silent-discharge-modified polypropylene film gave rise to three sets of peaks: those characteristic of the etched silver substrate; those due to cationized Irganox 1076; and an envelope of peaks between ∼*m/z* 500 and 1400 (Figure 11). Again each cluster pattern repeats at intervals of mass equal to that of CH_2 and the two most prominent components are separated by a mass equal to ^{109}Ag−^{107}Ag. These peaks can be assigned the generic formula $(CH_2)_nOAg^+$ on the basis of accurate mass measurement (the presence of the antioxidant $[M + Ag]^+$ peaks at *m/z* 637 and 639 was

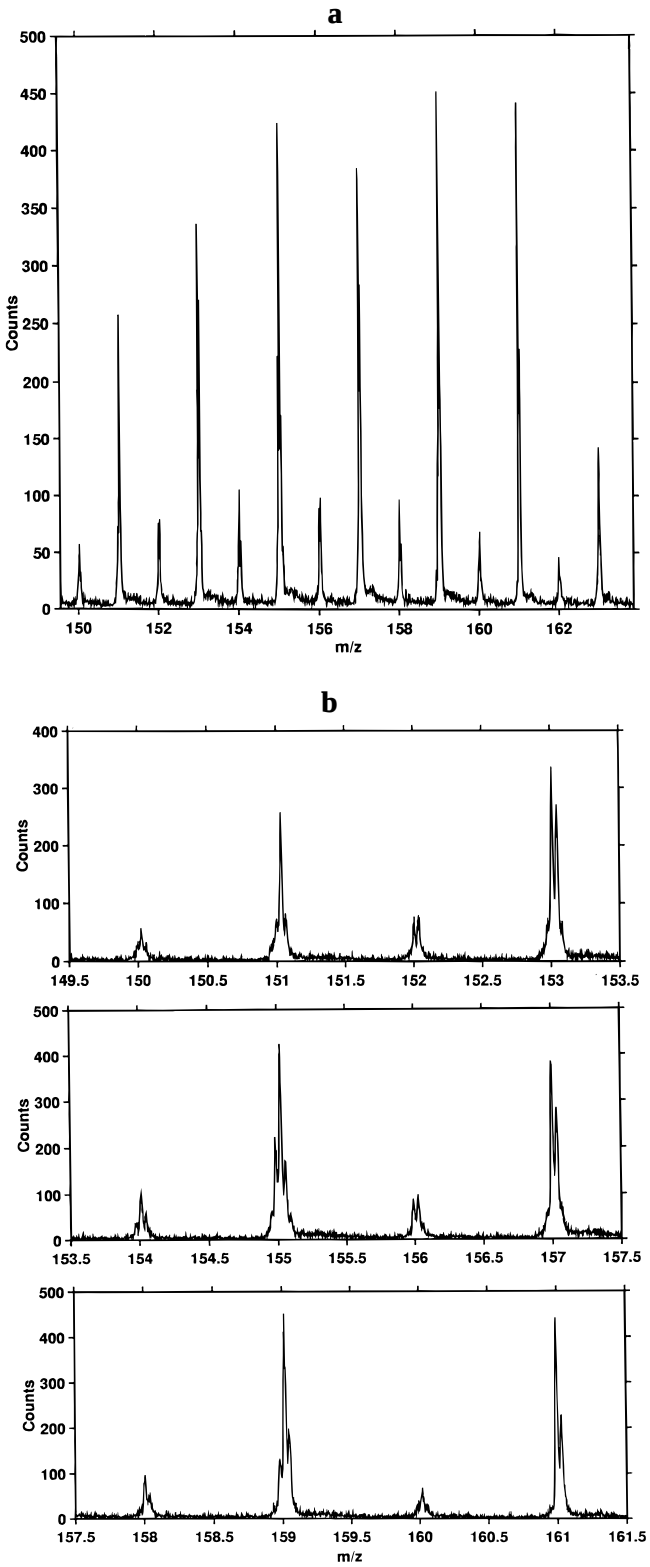

Figure 10. Representative details of cluster composition in Figure 8b: (a) intensity pattern with the cluster centered on *m/z* 157; (b) resolved components at each nominal mass.

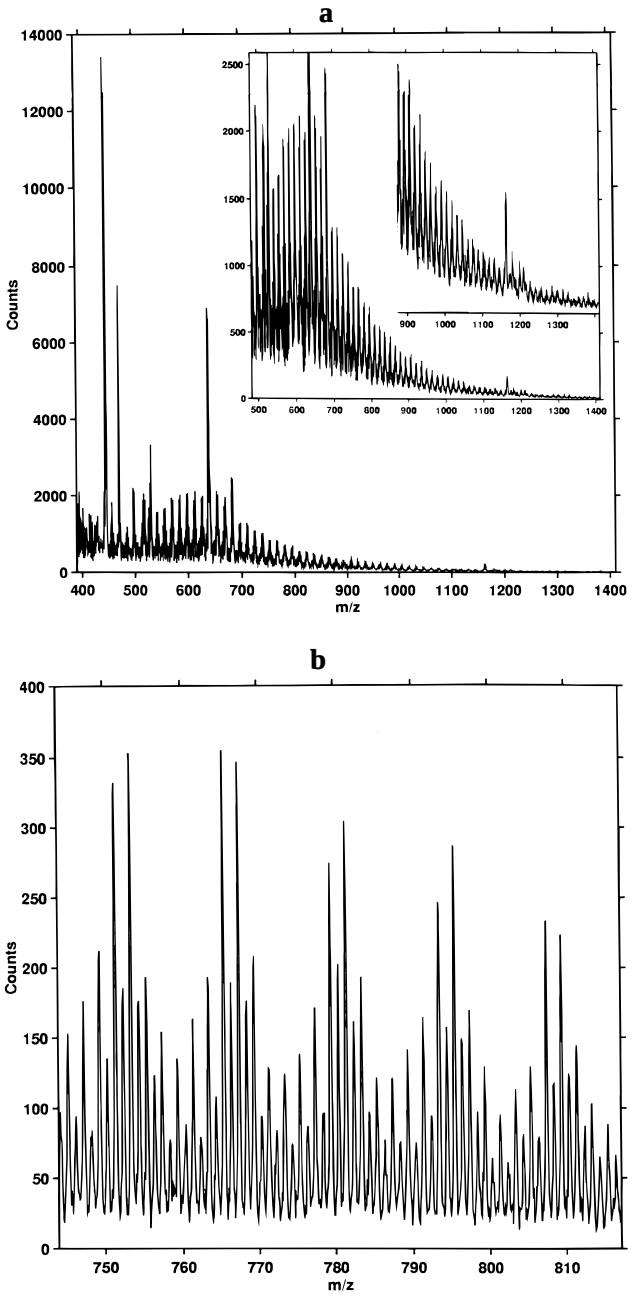

Figure 11. (a) Partial positive TOF-SIMS of chloroform extract from treated film deposited as a submonolayer onto etched silver foil showing the cationized oligomer distribution between *m*/*z* 500 and 1400 (the peak at ~*m*/*z* 1160 has not been assigned); (b) detail of representative clusters.

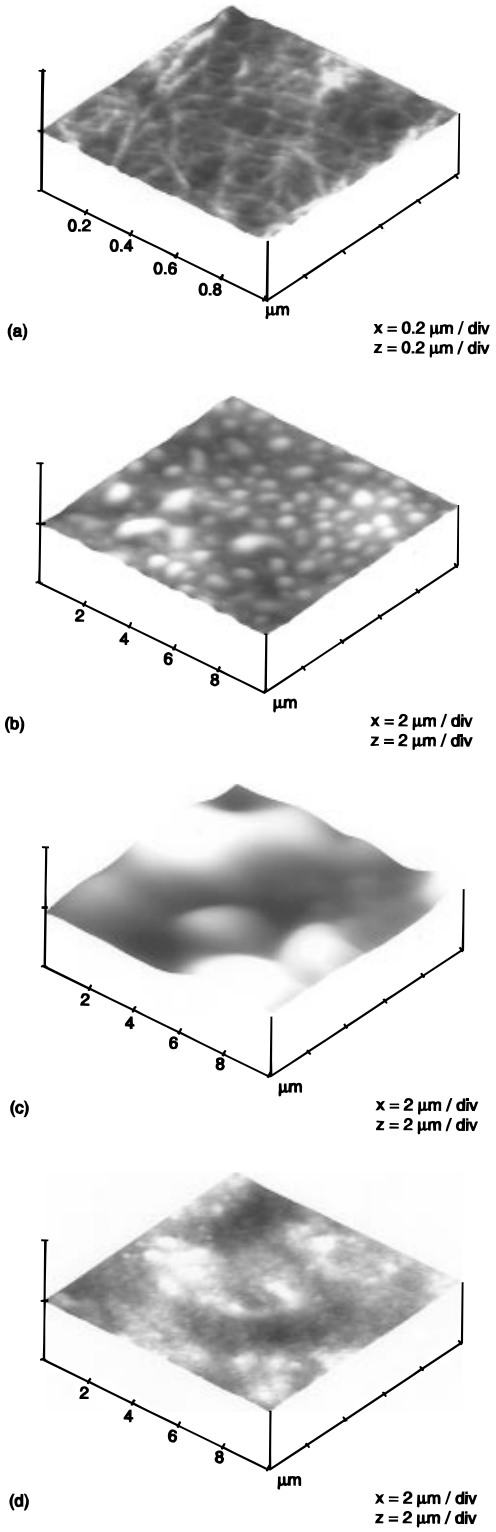

Figure 12. AFM images of silent-discharge-treated polypropylene: (a) untreated; (b) 30 s; (c) 240 s; (d) solvent washed (c).

helpful in this respect). The envelope may therefore be due to functionalized low molecular weight material resulting from oxidative chain scission of the polypropylene backbone. The highest mass clusters observed correspond to chains involving up to 100 carbon atoms. Such long hydrocarbon chains functionalized with one oxygen atom are consistent with the observations made by XPS and NMR analysis.

3.4. Atomic Force Microscopy. During polypropylene film manufacture, a long polymer tube is drawn and cooled to produce orientation along the drawing direction; the film is then reheated and blown outward with gas to form a bubble, which causes the polymer to also become oriented parallel to the bubble surface and thus perpendicular to the original tube drawing direction.[33] The overall effect is to produce a biaxial orientation, which can be seen by AFM as consisting of a fibrillar structure, with fibrils of the polymer oriented in two mutually orthogonal directions corresponding to the biaxial orientation introduced during the film blowing process (Figure 12). Polypropylene films prepared by this method tend to be highly crystalline;[34] however, the AFM micrographs do not reveal any spherulitic structure (Figure 12); this suggests that the crystalline spherulites are situated beneath the surface of the polymer film, as reported previously.[35,36]

There is a clear difference in topographical appearance between the untreated and silent-discharge-treated polypropylene surfaces. The fibrillar structure of bi-

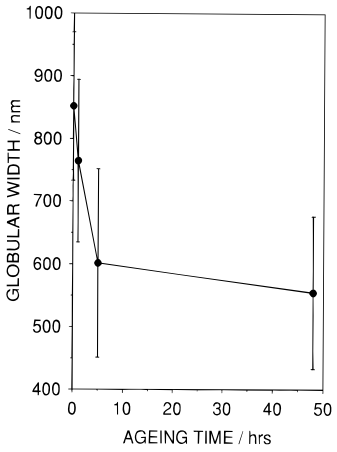

Figure 13. Variation in an average globule size for 30 s silent-discharge-treated polypropylene as a function of the aging period.

axially oriented polypropylene is lost, to be replaced by large globular type features (0.5−1.0 μm in diameter); these increase in size with longer treatment times (Figure 12). Washing the silent-discharge-treated polypropylene film in a 50/50 mixture of isopropyl alcohol and cyclohexane causes the disappearance of the globular features; this is consistent with the treated material being soluble low molecular weight species. However, the solvent-washed surfaces do not display the biaxial orientation seen previously for the untreated polymer; instead much smaller globular features are evident with diameters of just a few hundred nanometers.

Aging studies of the dielectric-barrier-treated polypropylene surfaces showed a gradual shrinking of the globular material with time (Figure 13). The areas analyzed by AFM were 100 μm^2, and the error bars shown in Figure 13 represent the average standard deviation taken from at least three experiments for each condition.

4. Discussion

The dielectric barrier discharge reactor was invented over a hundred years ago,[37] and both the chemistry and physics governing this type of nonequilibrium plasma has been widely studied.[38,39] A variety of reactive species are known to be produced in the presence of air; these include electrons, oxygen atoms, ozone, and ultraviolet radiation. Such a reactive medium can initiate polymer oxidation via chain scission, hydrogen abstraction, and oxygen attachment processes, leading to the formation of low molecular weight oxidized material (LMWOM),[13,40] which can be removed by solvent extraction.[41,42] The small amounts of NO_x species detected by TOF-SIMS have also been identified on discharge-treated surfaces by MIRS[43] and XPS.[40] The globular features observed by AFM can be attributed to the agglomeration of the LMWOM caused by the difference in surface energies between the LMWOM and the untreated polymer,[44,45] since it is energetically unfavorable for high surface energy substances to interact with low surface energy olefinic polymers.[46] It is important to note that, despite a gradual leveling off in the chemical composition of the plasma-treated surface layer, the LMWOM globules continue to expand in size with exposure time (Figures 2 and 12, respectively). These observations can help to rationalize the reported variability in performance of plasma-treated polymers for adhesive applications, since overtreatment can lead to excessive LMWOM and the formation of a weak interfacial layer despite the treated surface exhibiting good wettability characteristics.

A variety of explanations have been put forward to account for the aging of plasma-treated polymers; these include migration of mobile species out of the polymer bulk,[47] rearrangement of the modified polymer,[48] reaction with the atmosphere of trapped reactive species which were introduced into the substrate during treatment,[49] and desorption of the more volatile constituents from the surface. Some or all of these mechanisms may be responsible for the aging behavior seen in the surface topography and O/C ratio. Furthermore, surface aging helps to explain why there can often exist a discrepancy in the measured adhesive strength of a plasma-treated surface; since clearly the time between plasma treatment and bonding is critical.

5. Conclusions

Atmospheric dielectric barrier treatment of biaxially oriented polypropylene in air leads to the formation of globular low molecular weight oxidized material (LMWOM). The appearance of such globular features can be accounted for in terms of the difference in surface energies between LMWOM and the underlying olefinic polymer substrate. This LMWOM is seen to gradually disappear from the treated polymer surface with time.

Acknowledgment. R.D.B. thanks ICI for financial support and EPSRC for provision of instrumentation during the course of this work. The authors thank Alan Bunn for helpful discussions.

References and Notes

(1) d'Agostino, R.; Cramarossa, F.; Illuzzi, F. *J. Appl. Phys.* **1987,** *61,* 2754.
(2) Strobel, M.; Corn, S.; Lyons, C. S.; Korba, G. A. *J. Polym. Sci., Polym Chem. Ed.* **1985,** *23,* 1125.
(3) McCaulley, J. A.; Goldberg, H. A. *J. Appl. Polym. Sci.* **1994**, *53*, 543.
(4) Hansen, R. H.; Pascale, J. V.; DeBenedictics, T.; Rentzepis, P. M. *J. Polym. Sci. A* **1965**, *3*, 2205.
(5) Morra, M.; Occhiello, E.; Garbassi, F. *Metallized Plast.* **1991**, *2*, 363.
(6) Morra, M.; Occhiello, E.; Gila, L.; Garbassi, F. *J. Adhes.* **1990**, *33*, 77.
(7) Strobel, J. M.; Strobel, M.; Lyons, C. S.; Dunatov, C.; Perron, S. J**.** *J. Adhes. Sci. Technol.* **1991**, *5*, 119.
(8) Hopkins, J.; Badyal, J. P. S. *J. Phys. Chem.* **1995**, *99*, 4261.
(9) Shard, A. G.; Badyal, J. P. S. *J. Phys. Chem.* **1991**, *95*, 9436.
(10) Petrat, F. M.; Wolany, D.; Schwede, B. C.; Wiedmann, L.; Benninghoven, A. *Surf. Interface Anal.* **1994**, *21*, 402.
(11) Adamson, A. W. *Physical Chemistry of Surfaces*; Wiley: New York, 1960.
(12) Coopes, I. H.; Griffen, K. J. *J. Macromol. Sci. Chem.* **1982**, *17*, 217.
(13) Strobel, M.; Dunatov, C.; Strobel, J. M.; Lyons, C. S.; Perron, S. J.; Morgen, M. C. J. *Adhesion. Sci. Technol.* **1989**, *3*, 321.
(14) Gerenser. L. J. *J. Adhes. Sci. Technol.* **1987**, *1*, 303.
(15) Binnig, G.; Quate, C. F.; Gerber, Ch. *Phys. Rev. Lett.* **1986**, *56*, 930.
(16) Magonov, S. N.; Sheiko, S. S.; Deblieck, R. A. C.; Moller, M. *Macromolecules* **1993**, *26*, 1380.
(17) Snetivy, D.; Vancso, G. J. *Polymer* **1994**, *35*, 461.
(18) Jandt, K. D.; Buhk, M.; Miles, M. J.; Petermann, J. *Polymer* **1994**, *35*, 2458.
(19) Hopkins, J.; Boyd, R. D.; Badyal, J. P. S. *J. Phys. Chem.* **1996**, *100*, 6755.
(20) Greenwood, O. G.; Boyd, R. D.; Hopkins, J.; Badyal, J. P. S. *J. Adhes. Sci. Technol.* **1995**, *9*, 311.
(21) Hopkins, J.; Badyal, J. P. S. *Macromolecules* **1994**, *27*, 5498.
(22) Reichlmaier, S.; Hammond, J. S.; Hearn, M. J.; Briggs, D. *Surf. Interface Anal.* **1994**, *21*, 739.
(23) Zhong, Q.; Inniss, D.; Kjoller, K.; Elings, V. B. *Surf. Sci.* **1993**, *290*, L688.
(24) Evans, J. F.; Gibson, J. H.; Moulder, J. F.; Hammond, J. S.; Goretzki, H. *Fresenius' Z. Anal. Chem.* **1984**, *319*, 841.

(25) Beamson, G.; Briggs, D. *High Resolution XPS of Organic Polymers. The Scienta ESCA300 Database*; Wiley: Chichester, U.K., 1992.
(26) Wells, R. K.; Badyal, J. P. S. *J. Polym. Sci., Polym. Chem. Ed.* **1992**, *30*, 2677.
(27) Derome, A. E. *Modern NMR Techniques for Chemistry Research*; Pergamon: Oxford, U.K., 1987.
(28) Tonelli, A. E. *NMR Spectroscopy and Polymer Microstructure: The Conformational Connection;* VCH: New York, 1989.
(29) Brown, D. W.; Floyd, A. J.; Sainsbury, M. *Organic Spectroscopy*; Wiley: Chichester, U.K., 1988.
(30) Cotton, N. J.; Bartle, K. D.; Clifford, A. A.; Dowle, C. J. *J. Appl. Polym. Sci.* **1993**, *48*, 1607.
(31) Heatley, F.; Zambelli, A. *Macromolecules* **1969**, *2*, 618.
(32) *The Wiley Static SIMS Library*; Wiley: Chichester, U.K., 1996.
(33) McCrum, N. G.; Buckley, C. P.; Buckwall, C. B. *Principles of Polymer Engineering*; Oxford University: Oxford, U.K., 1988.
(34) Paulos, J. P.; Thomas, E. L. *J. Appl. Polym. Sci.* **1980**, *25*, 15.
(35) Norton, D. R.; Keller A. *Polymer* **1985**, *26*, 704.
(36) Aboulfaraj, M.; Ulrich, B.; Dahoun, A.; G'Sell, C. *Polymer* **1993**, *34*, 4817.
(37) Siemens, W. *Ann. Phys. Chem.* **1857**, *102*, 66.
(38) Eliasson, B.; Hirth, M.; Kogelschatz, U. *J. Phys. D: Appl. Phys.* **1987**, *20*, 1421.
(39) Eliasson, B.; Kogelschatz, U. *IEEE Trans. Plasma Sci.* **1991**, *19*, 309.
(40) Briggs, D.; Kendall, C. R.; Blythe, A. R.; Wootton, A. B. *Polymer* **1983**, *24*, 47.
(41) Xiao, G. Z. *J. Mater. Sci. Lett.* **1995**, *14*, 761.
(42) Lee, S. H. *J. Colloid Interface Sci.* **1995**, *14*, 761.
(43) Blythe, A. R.; Briggs, D.; Kendall, C. R.; Rane, D. G.; Zichy, V. J. I. *Polymer* **1978**, *19*, 1273.
(44) Greenwood, O. G.; Badyal, J. P. S. *Macromolecules* **1997**, *30*, 1091.
(45) Boyd, R. D.; Badyal, J. P. S. *Macromolecules* **1997**, *30*, 3658.
(46) Cherry, B. W. *Polymer Surfaces*; Cambridge University: Cambridge, U.K., 1981; p18.
(47) Occhiello, E.; Morra, M.; Cinquina, P.; Garbassi, F. *Polymer* **1992**, *33*, 3007.
(48) Garbassi, F.; Morra, M.; Occhiello, E.; Barino, L.; Scordamaglia, R. *Surf. Interface Anal.* **1989**, *14*, 585.
(49) Kuzuya, M.; Noguchi, A.; Ito, H.; Kondo, S.-I.; Noda, N. *J. Polym. Sci., Polym. Chem. Ed.* **1991**, *29*, 1.

MA960940X